Defence Science Journal, Vol. 70, No. 1, January 2020, pp. 72-81, DOI : 10.14429/dsj.70.14119

Simplified Motion Control of a Vehicle-manipulator for the Coordinated Mobile Manipulation

Swati Mishra[*,#], Santhakumar Mohan[@], and Santosh Kumar Vishvakarma[#]

[#]*Indian Institute of Technology, Indore - 453 552, India*
[@]*Indian Institute of Technology, Palakkad - 678 557, India*
[*]*E-mail: phd1501181004@iiti.ac.in*

ABSTRACT

This paper considers a resolved kinematic motion control approach for controlling a spatial serial manipulator arm that is mounted on a vehicle base. The end-effector's motion of the manipulator is controlled by a novel kinematic control scheme, and the performance is compared with the well-known operational-space control scheme. The proposed control scheme aims to track the given operational-space (end-effector) motion trajectory with the help of resolved configuration-space motion without using the Jacobian matrix inverse or pseudo inverse. The experimental testing results show that the suggested control scheme is as close to the conventional operational-space kinematic control scheme.

Keywords: Vehicle-manipulator system; Kinematically redundant system; Resolved motion control; Operational-space control

1. INTRODUCTION

In the current scenario, vehicle-manipulator systems have ample capabilities in the field of service robotics in specific space, underwater, building construction and social environments. Commercial industries are focusing on service robots to fulfil the need of customers and have become a topic of research nowadays. For enormous warehouses vehicle-manipulator system can be used as a service robot which comprises of a vehicle base and a manipulator arm. The objective of the warehouse automation is to perform a repeated task of picking an item from the warehouse and placing to the desired location to deliver with variability in the shipping orders. Hence, the vehicle-manipulator must follow a given desired well-defined path and trajectory. Various control schemes have been applied by the researchers and reported in the literature with different levels of success.

- However, controlling the operational-space pose vector, (i.e., end-effector positions and orientations) in a desired manner is always a difficult task.
- Moreover, the operational-space pose sensor is an expensive one and getting an exact measurement is also difficult due to the limitations of inertial measurements and available technologies.
- Further, getting an exact end-effector pose information from the help of an internal global position system (IGPS) is an alternative option, however, it is quite complex, expensive and not feasible to have at the warehouses and other service-oriented outdoor environment[1].

Received : 11 February 2019, Revised : 10 May 2019
Accepted : 21 May 2019, Online published : 10 February 2020

Therefore, several researchers often try to use the inverse kinematic solution based on conventional configuration-space control schemes, however, most of the vehicle-manipulator systems are kinematically redundant systems, i.e., the number of configuration (controllable) variables are more the required degrees of freedom (number of end-effector associated variables). So, solving the inverse kinematic problem of a kinematically redundant system is too difficult and has multiple solutions[1]. Further, in this connection, there are several inverse kinematic solving techniques and solvers like different first order methods to solve kinematic redundancy are proposed as discussed[2-3].

The literature reveals that the existing research has been focused on motion control design algorithms for the trajectory tracking performance of the fixed manipulators. Therefore, redundancy resolution scheme remains a challenging problem for the robotic researchers[3]. According to kinematic control scheme[4-6] based on the inverse kinematic transformation and pseudo inverse is proposed which helps in solving the problem of redundancy. In the presence of kinematics and dynamics along with the input disturbances, a task-space tracking control is suggested[7]. The kinematic control algorithm is implemented and is effectively demonstrated by numerical simulations[8,9]. For manipulation of an object, a proper coordinated motion is required for the robot arm, so reference[10] demonstrates a new control algorithm in this direction. The work[11] involves the use of pseudo-inverse of the Jacobian matrix and obtains the accurate joint solutions because of using the direct inverse kinematic solutions. The suggested[12,13] controller compensates the uncertainties and validates the stability of the system by

converging to all the errors to zero with the help of Lyapunov's direct method. In[14,15], the results show the task priority redundancy resolution using the matrix inversion approach based on the damped least squares. In recent days there is an emerging technique of reinforcement learning which is attractive to the robotic researchers. In this connection, even kinematic control of a vehicle-manipulator through the help of reinforcement learning has been done in the recent past[16-18].

Redundant robots need larger flexibility and higher efficiency for manipulation point of view. Due to non-availability of proper kinematics, computation is a problem. But from the computational point of view, these techniques require very high computing facilities and implicate an expensive system.

- Controlling mobile manipulation using Pseudo Inverse provides eventually better performance. However, the use of Pseudo Inverse is an expensive solution for low cost micro-controllers.

Researchers are also working towards the visual based control of vehicle-manipulators[19-21]. But it involves complex image processing algorithms which are computationally expensive and cannot be deployed on a low-cost micro-controller. Similarly, deploying an operational-space kinematic control with the help of Moore-Penrose pseudo-inverse[22] of the Jacobian matrix may produce a traceable path, however, in certain occasions the vehicle and the manipulator motions are intersecting. Therefore, it requires proper joint limitation to the manipulator arm.

A resolved motion kinematic control scheme is recommended in such a way that the mobile base (vehicle) and the manipulator actuation are utilised effectively and achieved dexterous mobile manipulation. In the proposed scheme the vehicle motion is decomposed in such a way that the vehicle coordinate frame and the end-effector frame is maintained with the minimum safe distance. The safe distance is decided based on the dexterous workspace of the manipulator arm. So, the vehicle position and orientation are obtained with the help of line of sight (LoS) motion control strategy with a minimum safe distance as per the manipulator arm characteristics. The manipulator arm joint positions are obtained through the help of closed-form inverse kinematic solution (which is available readily) based on the vehicle position and its orientation along with the desired operational-space pose vector. The focus of the paper is related to coordinate motion control of a vehicle-manipulator system. Therefore, the desired operational-space is resolved as desired configuration-space variables of the vehicle-manipulator. To certify the suggested control, scheme the computed velocity control law is applied on a real time vehicle- manipulator, namely, JR2 and compared with the conventional operational-space control scheme. Hence the main contribution of the paper is to propose as mentioned above, in this paper, a novel kinematic control scheme and its overall performance is compared to the conventional operational-space control scheme. To get an optimal solution, it is mandatory to employ some constrained optimisation techniques and few of them are approached in this manner and they are available in the literature[23-28].

2. SYSTEM DESCRIPTION

In this work, the mobile manipulator considered for the analysis constitutes a six-link serial manipulator anchored on a four-mecanum wheeled mobile platform. The photo and the kinematic frame arrangement of the mobile manipulator is as shown in Fig. 1 where, O (0, 0, 0) is the earth-fixed inertial frame, B $(x_{B,}y_{B,}z_{B})$ is the mobile base (moving) frame and $T(x_t, y_t, z_t)$ is the end-effector frame. $\eta \in \Re^{9\times1}$ is the vector of configuration (joint) space position variables, $\eta = [\eta_v \quad \eta_m]^T$. $\eta_m \in \Re^{3\times1}$ is the vector of mobile base positions and orientation and given as: $\eta_v = [x \quad y \quad \psi]^T$;

$\eta_m \in \Re^{6\times1}$ is the vector of manipulator rotary joint angles and given as: $\eta_m = [\theta_1 \quad \theta_2 \quad \theta_3 \quad \theta_4 \quad \theta_5 \quad \theta_6]^T$; *u, v* and *r* are the mobile base translation positions and the heading (yaw) angular displacement. θ_1, θ_2 and θ_3 are the manipulator joint angles of the interrelated serial manipulator links. $\dot{\eta} \in \Re^{6\times1}$ is the vector of configuration space velocities. $\xi = [\xi_b \quad \xi_m]^T \in \Re^{9\times1}$ is the vector of control inputs in body-fixed coordinate frame stated as: $\xi = [u \quad v \quad r \quad \dot{\theta}_1 \quad \dot{\theta}_2 \quad \dot{\theta}_3 \quad \dot{\theta}_4 \quad \dot{\theta}_5 \quad \dot{\theta}_6]^T$, where $\xi_b \in \Re^{3\times1}$ is the vector of inputs of the mobile basestated as: $\xi_b = [u \quad v \quad r]^T$ and $\xi_m \in \Re^{6\times1}$ is the vector of input torques of the serial manipulator mounted on a mobile base given as: $\xi_m = [\dot{\theta}_1 \quad \dot{\theta}_2 \quad \dot{\theta}_3 \quad \dot{\theta}_4 \quad \dot{\theta}_5 \quad \dot{\theta}_6]^T$.

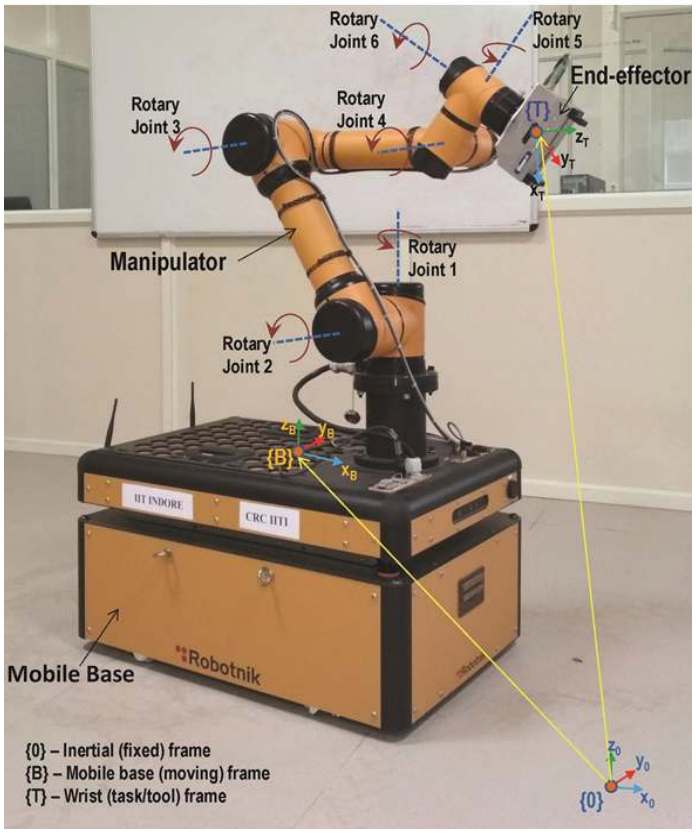

Figure 1. Kinematic frame arrangement of the JR2 mobile manipulator.

3. KINEMATIC MODEL OF THE VEHICLE-MANIPULATOR

The suggested mobile manipulator constitutes 3 degree of freedom (dof) of mobile base and a 6-dof serial manipulator. The joint frame arrangement and the robot configuration are as described in Fig. 2.

The desired motion of the manipulator is considered and represented in the Cartesian (task) space. The operational-space position, velocity and acceleration vectors can be insinuated as:

$$\rho = fun(\eta) \tag{1}$$

where, $\rho = [x \quad y \quad z \quad \alpha \quad \beta \quad \gamma]^T$ is the operation-space pose vector, in other words, the vector of the end-effector positions and orientations. $\eta = [x_v \quad y_v \quad \theta_v \quad \theta_1 \quad \theta_2 \quad \theta_3 \quad \theta_4 \quad \theta_5 \quad \theta_6]^T$ is the vector of the configuration-space position variables. the configuration-space velocity vector can be expressed as follows:

$$\dot{\eta} = J_1(\eta)\xi \tag{2}$$

where, $\dot{\eta} = [\dot{x}_v \quad \dot{y}_v \quad \dot{\theta}_v \quad \dot{\theta}_1 \quad \dot{\theta}_2 \quad \dot{\theta}_3 \quad \dot{\theta}_4 \quad \dot{\theta}_5 \quad \dot{\theta}_6]^T$ is the vector of the inertial frame (earth-fixed) configuration-space velocities. $\xi = [u \quad v \quad r \quad \dot{\theta}_1 \quad \dot{\theta}_2 \quad \dot{\theta}_3 \quad \dot{\theta}_4 \quad \dot{\theta}_5 \quad \dot{\theta}_6]^T$ is the vector of the vehicle-frame fixed configuration-space velocities. $J_1(\eta) \in \Re^{9\times 9}$ is the vehicle Jacobian matrix which maps the configuration-space velocities from the body-fixed frame to the inertial frame. Forward velocity model or the differential kinematic model of the vehicle manipulator system can be expressed by differentiating (1) with respect to time, as follows:

$$\begin{aligned} \dot{\rho} &= J_2(\eta)\dot{\eta} \\ \dot{\rho} &= J_2(\eta)J_1(\eta)\xi = J(\eta)\xi \end{aligned} \tag{3}$$

where, $\dot{\rho} = [\dot{x} \quad \dot{y} \quad \dot{z} \quad \dot{\alpha} \quad \dot{\beta} \quad \dot{\gamma}]^T$ is the vector of the operational-space velocities, in other words, the vector of the end-effector linear and angular velocities. $J_2(\eta) \in \Re^{6\times 9}$ is the end-effector Jacobian matrix which maps the end-effector velocities to the inertial frame configuration-space velocities. $J(\eta) \in \Re^{6\times 9}$ is the Jacobian matrix which maps the end-effector (operational-space) velocities to the vehicle-fixed frame (configuration-space) velocities.

3.1 Actuator Input Allocation

As the system is heterogeneous comprises of a four wheel mobile base with their own wheel velocities and a manipulator with six angular rotary joints with their own input joint velocities. To correlate the generalised input velocity vector with the individual actuator inputs (rotational speeds) of the proffered kinematically redundant system, the input (control) vector can be rewritten as follows:

$$\begin{aligned} \xi &= W\kappa \\ \kappa &= W^{+}\xi \end{aligned} \tag{4}$$

where, W is the actuator configuration matrix and κ is the vector of actuator velocity inputs. Here, W^+ is the weighted pseudo matrix inverse and it can be modified based on the configuration and requirements. The weighted matrix used for the weighted pseudo inverse is a diagonal matrix and its diagonal values lie between 0 to 1.

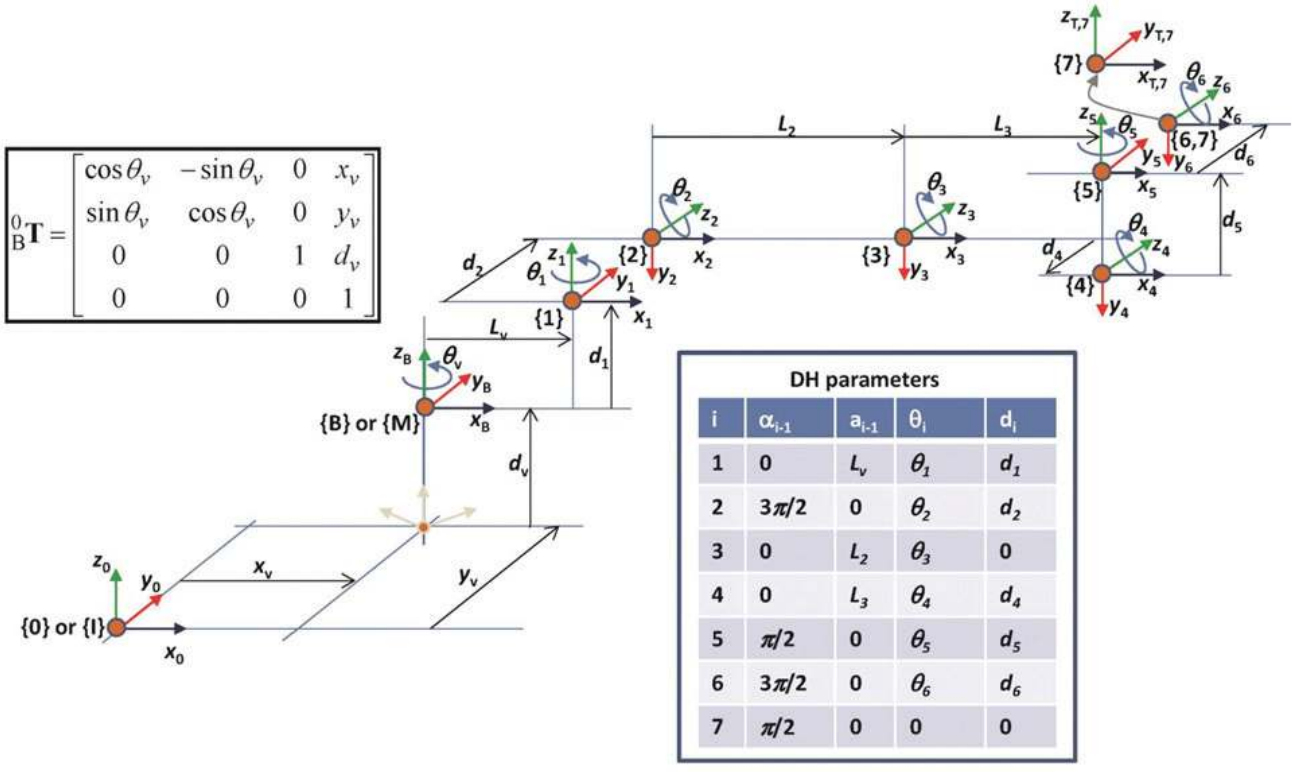

i	α_{i-1}	a_{i-1}	θ_i	d_i
1	0	L_v	θ_1	d_1
2	$3\pi/2$	0	θ_2	d_2
3	0	L_2	θ_3	0
4	0	L_3	θ_4	d_4
5	$\pi/2$	0	θ_5	d_5
6	$3\pi/2$	0	θ_6	d_6
7	$\pi/2$	0	0	0

Figure 2. The systematic frame arrangement along with kinematic parameters of the JR2 mobile manipulator as per the Denavit-Hartenberg representation.

4. KINEMATIC CONTROL DESIGN

In this research computed velocity control is implemented to achieve the aim to follow the desired operational space pose vector trajectory of the vehicle manipulator with uncertainties and time varying external disturbances. The control law used in the research article can be discussed as:

4.1 Conventional Operational-space Velocity Control

$$\xi = J(\eta)^{+}\left(\dot{\rho}_d + K\tilde{\rho}\right) \tag{5}$$

where $J(\eta)^{+} \in \Re^{9\times 6}$ is the pseudo inverse of the Jacobian matrix. Jacobian is a non-square matrix. As it is a task space kinematic control so $J(\eta)$ need to be inverted. Hence, we are using Moore–Penrose inverse. $\dot{\rho}_d$ is the vector of desired operational-space velocities. $\tilde{\rho} = \rho_d - \rho$ is the vector of operational-space pose errors. ρ_d is the desired operational space pose vector. ρ is the actual operational-space pose vector. K is the controller gain matrix and chosen as a symmetric positive definite matrix, that is, $K = K^T > 0$.

4.2 Resolved Operational-space Motion to the Configuration-space Velocity Control

$$\xi = J_1(\eta)^T\left(\dot{\eta}_d + \Lambda\tilde{\eta}\right) \tag{6}$$

where $J_1(\eta)^T = J_1(\eta)^{-1} \in \Re^{9\times 9}$ is the inverse of the vehicle Jacobian matrix. $\dot{\eta}_d$ is the vector of desired inertial frame (earth-fixed) configuration-space velocities which is obtained from the desired operational-space velocities. $\tilde{\eta} = \eta_d - \eta$ is the vector of configuration-space pose errors. η_d is the desired configuration-space pose vector which is resolved from the operational-space pose vector. η is the actual configuration-space pose vector. Λ is the controller gain matrix and chosen as a symmetric positive definite matrix, i.e. $\Lambda = \Lambda^T > 0$

$$\eta_d = \begin{bmatrix} \eta_{dv} \\ \eta_{dm} \end{bmatrix} \tag{7}$$

where, $\eta_{dv} = \begin{bmatrix} x_{dv} & y_{dv} & \theta_{dv} \end{bmatrix}^T$ is the vector of desired positions and orientation of the vehicle. $\eta_{dm} = \begin{bmatrix} \theta_{1dm} & \theta_{2dm} & \theta_{3dm} & \theta_{4dm} & \theta_{5dm} & \theta_{6dm} \end{bmatrix}^T$ is the vector of desired joint angles of the spatial manipulator arm. In this work, it is resolved in two steps, the first step is finding the vehicle positions and orientation with the help of line of sight method and the second step is finding the inverse kinematic solutions of the spatial manipulator. The vector of desired positions and orientation of the vehicle can be obtained as follows:

$$\begin{aligned} \theta_{vd} &= a\tan 2\left(\dot{y}_d, \dot{x}_d\right) \\ x_{vd} &= x_d - R_{\min}\cos\theta_{vd} \\ y_{vd} &= y_d - R_{\min}\sin\theta_{vd} \end{aligned} \tag{8}$$

where, $R_{\min}$ is the minimum safe radial distance between the vehicle frame and the end-effector frame. The vector of desired joint angles of the manipulator can be obtained as follows:

$$\eta_{dm} = fun(\mu) \tag{9}$$

where, μ is the manipulator pose vector from its base frame. Further, it can be expressed as per the proposed method as follows:

$$\mu = \begin{bmatrix} \left(R_{\min} - l_v\right)\cos\theta_{vd} \\ \left(R_{\min} - l_v\right)\sin\theta_{vd} \\ z_d - d_v \\ \alpha_d \\ \beta_d \\ \gamma_d \end{bmatrix} \tag{10}$$

4.3 Stability Analysis

The proposed controller closed loop asymptotic stability is verified by Lyapunov direct method in which following assumptions are assumed:

Assumption 1: The controller and observer gain matrices and chosen as a symmetric positive definite matrix which is given as: $x^T\Lambda x = x^T\Lambda^T x > 0$, $x^T K x = x^T K^T x > 0$, or simply

$$\Lambda = \Lambda^T > 0; K = K^T > 0;$$

Further, the gain matrices are assumed to be positive diagonal matrices for simplicity, as follows:

$$\Lambda = k_1 I_{9\times 9}; K = k_2 I_{6\times 6};\ \ k_1 > 0, k_2 > 0; \tag{11}$$

Assumption 2: The total lumped disturbance vector value is arbitrarily large, bounded and slowly varying with time i.e. $\dot{\rho}_{dis} \approx 0$.

The system is bounded to follow the given operational-space position trajectory and the desired operational-space trajectory is considered as ρ_d. So, Lyapunov candidate function is:

$$V_1(\tilde{\eta}) = \frac{1}{2}\tilde{\eta}^T\tilde{\eta} \tag{12}$$

Further differentiating with respect to time along with state trajectories, it gives,

$$\dot{V}_1(\tilde{\eta}) = \tilde{\eta}^T\dot{\tilde{\eta}} \tag{13}$$

$$\dot{\eta} = J_1(\eta)\xi \tag{14}$$

$$\xi = J^{-1}(\eta)[\dot{\eta}_d + k_1\tilde{\eta}] \tag{15}$$

$$\dot{\tilde{\eta}} = \dot{\eta}_d - [\dot{\eta}_d + k_1\tilde{\eta}] = -k_1\tilde{\eta} \tag{16}$$

Substituting (16) in (13), it becomes

$$\dot{V}_1(\tilde{\eta}) = -\tilde{\eta}^T k_1\tilde{\eta} \tag{17}$$

Lyapunov candidate function for the conventional operational-space control scheme, as follows:

$$V_2(\tilde{\mu}) = \frac{1}{2}\tilde{\rho}^T\tilde{\rho} \tag{18}$$

After differentiating with respect to time along with state trajectories, it gives,

$$\dot{V}_2(\tilde{\mu}) = \tilde{\rho}^T\dot{\tilde{\rho}} \tag{19}$$

Operational space velocity errors which is stated as:

$$\dot{\tilde{\rho}} = \dot{\tilde{\rho}} - \dot{\rho} \tag{20}$$

$$\dot{\rho} = J_1(\eta)\xi = J_2(\eta)\dot{\eta} \tag{21}$$

$$\dot{\rho} = J_2(\eta)J_1(\eta)\xi = J(\eta)\xi \tag{22}$$

$$\xi = J^{+}(\eta)[\dot{\rho}_d + k_2\tilde{\rho}] \tag{23}$$

Substituting (23) in (19), it becomes

$$\dot{V}_2(\tilde{\mu}) = -(\tilde{\rho}^T k_2 \tilde{\rho}) \tag{24}$$

The Lyapunov candidate function's time derivatives are negative definite which means that chosen control designs are globally asymptotically stable and the tracking errors converge to zero asymptotically. The controller parameters of the controller schemes, namely, k_1 and k_2 .

5. TESTING AND OUTCOMES

To validate the usefulness of the suggested motion control design, a performance investigation of the mobile manipulator's operational-space position tracking is executed by extensive numerical simulations in the MATLAB/Simulink package. The proffered vehicle manipulator comprises of 6-dof manipulator attached on a 3-dof vehicle platform. The specifications of the mobile manipulator which are used for this study are as presented in Table 1.

The photo of the JR2 mobile manipulator along with its kinematic control package, namely, the MoveIt software in the lab environment is as shown in Fig. 3. To validate the conventional system, four profiles have been taken.

Table 1. Technical specifications and parameters of the JR2 mobile manipulator

Specification / Parameter	Value
Size of the mobile base	800 mm × 550 mm × 420 mm
Maximum speed of the mobile base	3 m/s
Number of wheels	4
Number of manipulator axes	6
Work envelope of the manipulator	0.629 m^3
Horizontal distance between the vehicle frame to the manipulator base (L_v)	0.3 m
Vertical distance between the vehicle frame to the manipulator base (d_1)	0.258 m
Vehicle frame from the ground (height) (d_v)	0.42 m
Joint distance of the manipulator's fourth frame (d_4)	0.109 m
Joint distance of the manipulator's fifth frame (d_5)	0.102 m
Joint distance of the manipulator's sixth frame (d_6)	0.0825 m
Length of the manipulator second link (L_2)	0.408 m
Length of the manipulator third link (L_3)	0.372 m

To show robustness and effectiveness it tracks four different spatial position trajectories as given in Figs. 4(a) eight-shaped trajectory 4(b) infinity-shaped trajectory 4(c) circular-shaped trajectory 4(d) square-shaped trajectory.

Figure 5 demonstrates sequence of flow between the system components of the JR2 vehicle-manipulator. The controller parameters of both schemes, namely, k and ω values are chosen as 5 and 4 in such a way that both controllers are

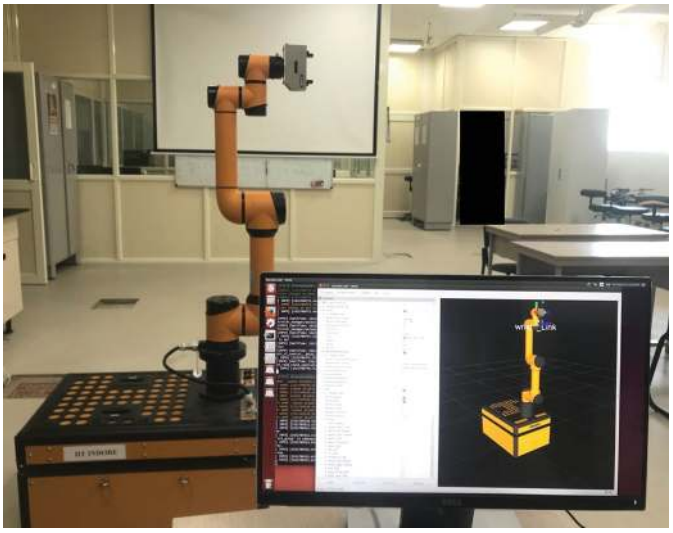

Figure 3. Photo of the JR2 mobile manipulator along with its kinematic control package, namely, the MoveIt software in the lab environment.

giving almost same performance in terms of error quantifiers. For better quantification, the values of root mean square (RMS) errors and integral-time of absolute errors (ITAE) have been recorded. Both control schemes are equivalent after initial transient point. The steady state behaviour is also equivalent. These proposed controller follows all the four patterns successfully which are used in commercial sector. In this article for analysing the trajectory performance following conventional operational space backstepping control scheme is used. For measuring the controller's performance, two error quantifiers are used in this article, namely, Integral Time of Absolute error and Root Mean Square Error. The error quantifier's act plays a significant role in measuring controller's performance. Integral Time of Absolute error integrates the absolute error multiplied by the time over time. It is the square root of the average of squared errors. Equation 25 calculates the end-effector position and orientation error values which is used in measuring performance quantifiers. Equation 26 calculates root mean square error values and Integral Time of Absolute error as shown follows:

$$\begin{aligned} \tilde{p} &= \sqrt{(x_d - x)^2 + (y_d - y)^2 + (z_d - z)^2} \\ \tilde{o} &= \sqrt{(\alpha_d - \alpha)^2 + (\beta_d - \beta)^2 + (\gamma_d - \gamma)^2} \end{aligned} \tag{25}$$

$$\begin{aligned} \tilde{x}_{rms} &= \sqrt{\frac{\sum_{i=1}^{n}(x_{di} - x_i)^2}{n}} \\ \tilde{x}_{itae} &= \int t\,|x_d - x|dt \end{aligned} \tag{26}$$

Figure 6 presents the desired operational-space positions trajectories along with time trend of the end-effector positions. Figure 7 depicts the desired operational-space positions trajectories along with time trend of the end-effector orientations. Figure 8 depicts time trend of the norm of operational-space position tracking errors under system dynamic variations (controller sensitivity results. The time trend of end-effector pose tracking errors is presented for

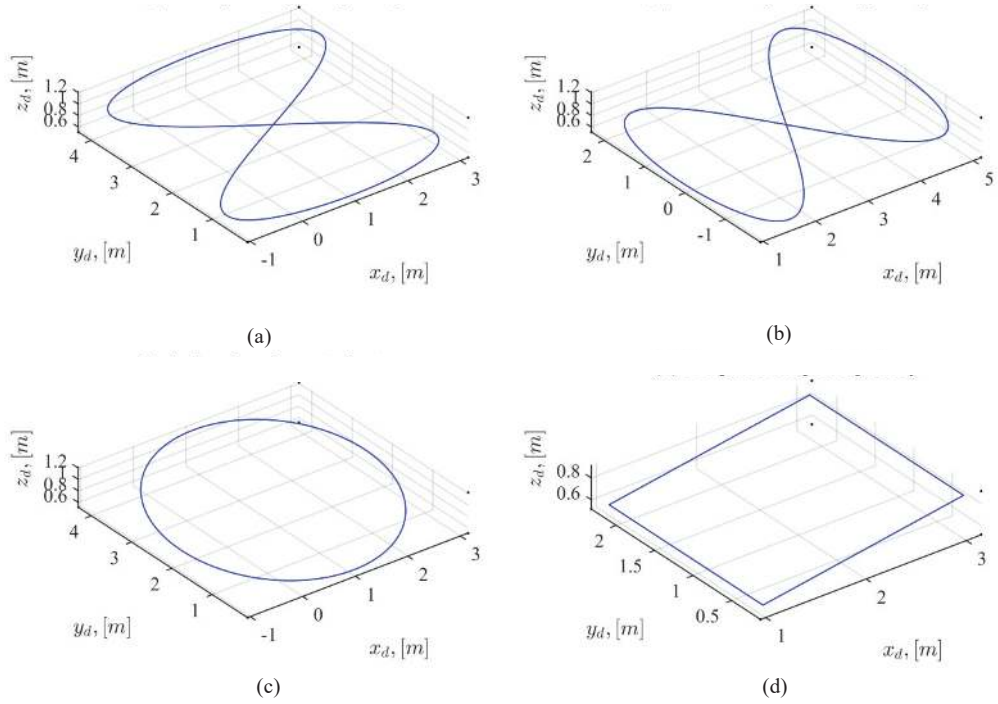

Figure 4. Desired complex spatial operational-space position trajectories for the performance evaluation: (a) An eight shape trajectory, (b) An infinity shape trajectory, (c) A circular shape trajectory, and (d) A square shape trajectory.

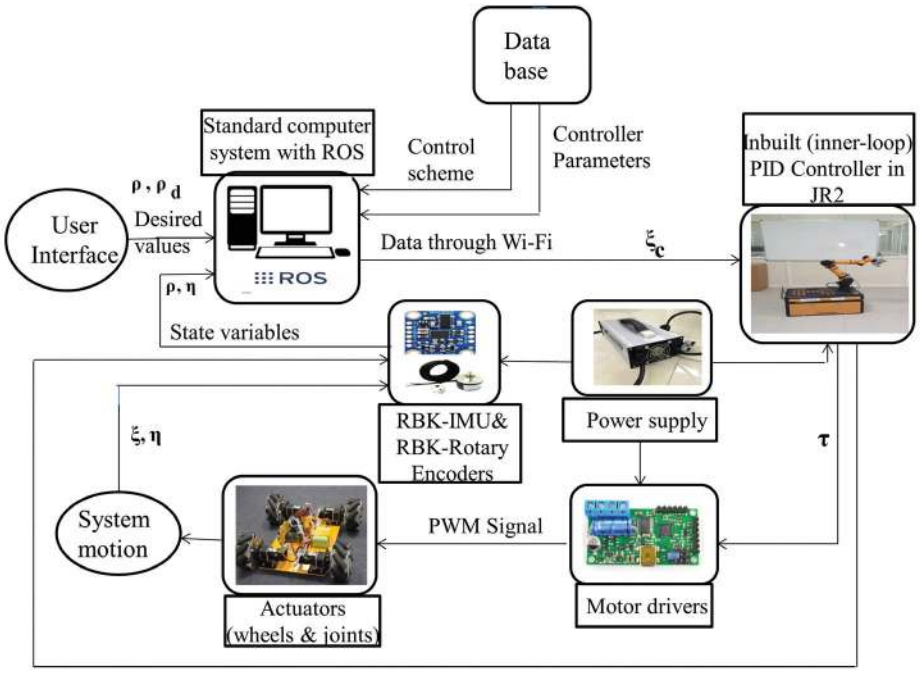

Figure 5. Sequence of flow between the components of the JR2 vehicle-manipulator in real-time working conditions.

the variations of the controller gain matrix values (here it is a scalar value); the scalar value is varied from 2 to 10 units. Controller gain sensitivity has been observed in terms of the end effector pose errors and it was found that the increase in controller gain (Λ) values giving faster convergence and value of steady state errors are decreasing. However, the actuator inputs are getting higher at the initial phase due to the faster convergence, therefore, it is considered the value based on the trade-off between both values of tracking errors, convergence rate and actuator inputs. The proposed controller has large error at initial stages due to the resolved motion in its task space; however, the conventional control scheme the errors are smaller at the initial stages as compared to the proposed scheme. Overall, the mean values of ITAE are as equal to the operational-space control scheme. The values of Λ, have been varied, the error quantifiers in terms of position and orientation errors are almost same at the steady states but the response time is varied, in fact, faster response obtained in the higher regions of gain values. However, in terms of the position error values, it is least when controller gain is 5 to 7 units and the orientation error values; it is least between 3 to 5 units. Table 2 describes the comparison of controller performances through quantifiers between the conventional operational- space kinematic control scheme and the proposed resolved motion kinematic control scheme in configuration-space. In the table, the operational space pose tracking errors for four desired complex trajectories are calculated and compared between the conventional operational-space kinematic control scheme and the proposed kinematic control scheme. This signifies that proposed new kinematic control scheme is successful in tracking the operational space position and performance. Further, based on experiments, it assured its closed-loop stability as well.

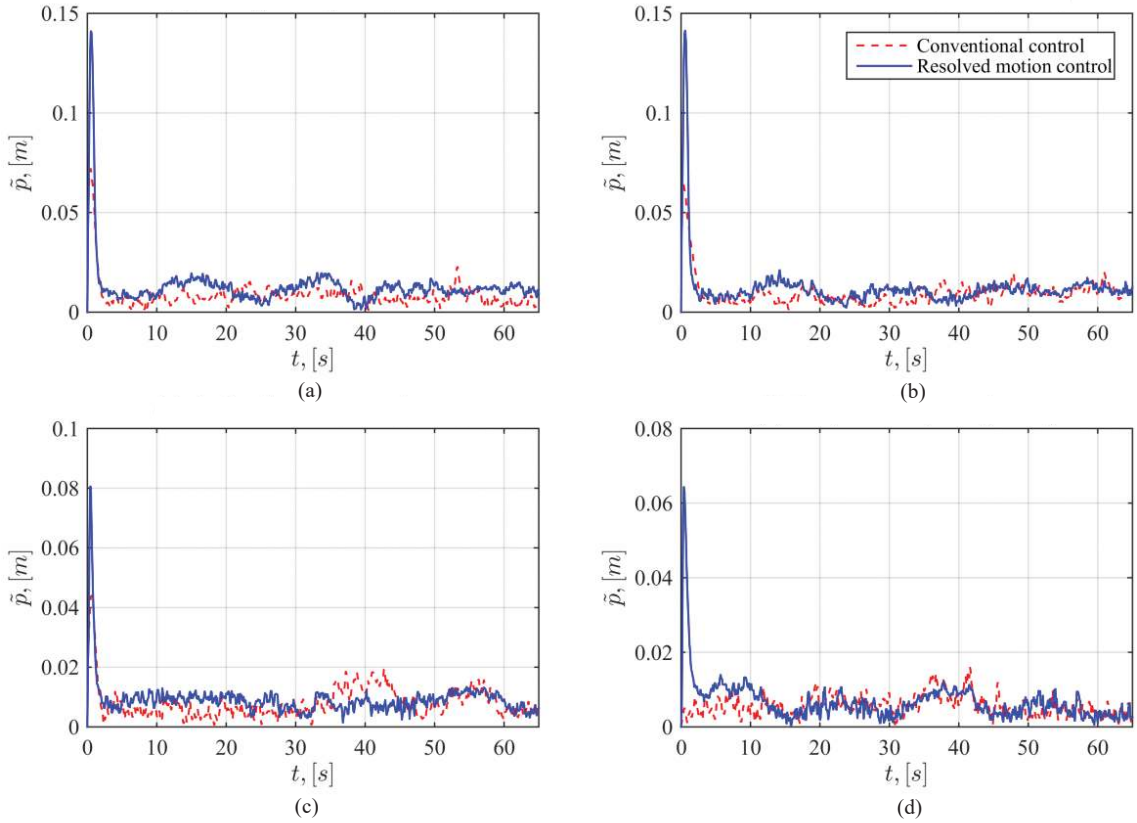

Figure 6. Desired operational-space positions trajectories along with time trend of the end-effector positions: (a) An eight shape trajectory, (b) An infinity shape trajectory, (c) A circular shape trajectory, and (d) A square shape trajectory.

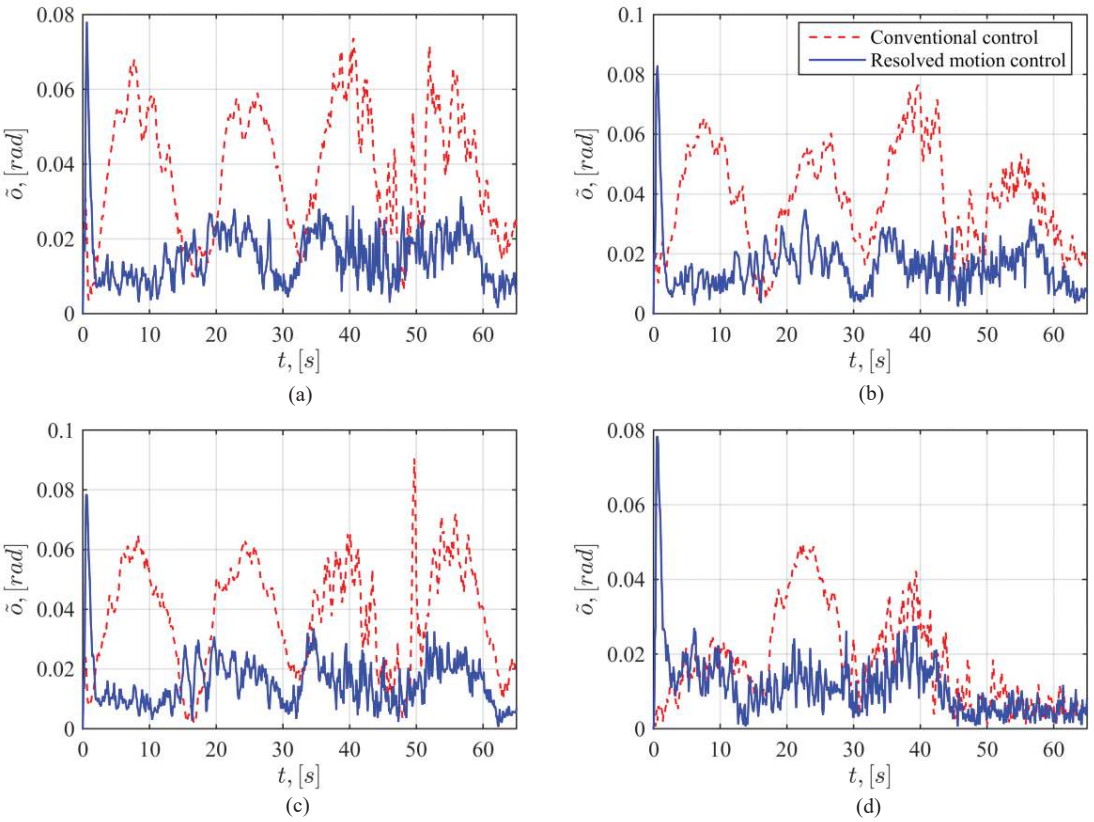

Figure 7. Desired operational-space positions trajectories along with time trend of the end-effector orientations: (a) An eight shape trajectory, (b) An infinity shape trajectory, (c) A circular shape trajectory, and (d) A square shape trajectory.

Table 2. Comparison of controller performance quantifiers between Conventional operational-space kinematic control scheme and Resolved motion kinematic control scheme in configuration-space

Parameter or performance quantifier	Conventional operational-space kinematic control scheme				Resolved motion kinematic control scheme in configuration-space			
	Eight shape	Infinity shape	Circular shape	Square shape	Eight shape	Infinity shape	Circular shape	Square shape
$\tilde{x}_{rms}$ in mm	9.8	7.6	7.6	4.1	15.1	9.1	7.2	3.9
$\tilde{y}_{rms}$ in mm	5.3	8.9	4.2	3.3	7.1	13.2	4.8	3.7
$\tilde{z}_{rms}$ in mm	3.5	3.1	4.6	3.4	7.3	7.5	7.1	7.3
$\tilde{\alpha}_{rms}$ in rad	0.030	0.029	0.030	0.014	0.008	0.009	0.008	0.006
$\tilde{\beta}_{rms}$ in rad	0.025	0.024	0.025	0.011	0.014	0.015	0.015	0.012
$\tilde{\gamma}_{rms}$ in rad	0.015	0.018	0.015	0.012	0.006	0.005	0.006	0.004
$\tilde{x}_{itae}$ in units	9.51	11.93	9.31	6.76	17.23	8.43	8.54	4.44
$\tilde{y}_{itae}$ in units	9.49	10.91	8.00	5.29	7.76	15.42	8.15	6.52
$\tilde{z}_{itae}$ in units	5.27	6.31	8.82	5.36	10.31	10.27	9.87	5.20
$\tilde{\alpha}_{itae}$ in units	58.93	54.76	60.76	17.53	14.65	14.92	14.05	8.29
$\tilde{\beta}_{itae}$ in units	26.85	25.82	27.29	12.22	23.20	23.03	22.85	11.64
$\tilde{\gamma}_{itae}$ in units	32.83	37.06	31.62	16.78	11.18	10.50	10.21	7.67

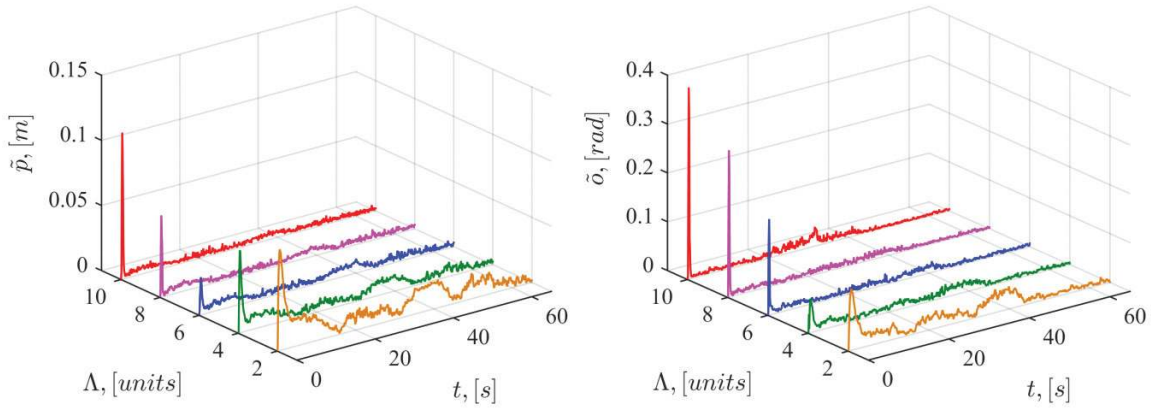

Figure 8. Time trend of the norm of operational-space position tracking errors under system dynamic variations (controller sensitivity results).

6. CONCLUSIONS

In this research article, a new resolved motion kinematic control scheme is proposed and compared with the conventional operational-space kinematic control scheme. The suggested new kinematic control scheme is successful in tracking the operational space position and performance when compared with the conventional scheme. The control scheme is demonstrated experimentally; it is effective and can be extended up to the dynamic motion control scheme as well. Further the motion control scheme simplifies the computability. Since the motion control scheme is effective so no need to use any advanced complex schemes like reinforcement learning, visual servoing and other complex resolution algorithms. The proposed end-effector motion trajectory is tracked with the help of resolved configuration-space motion without using the Jacobian matrix inverse. So, the system becomes stable and tracking errors are also converging to zero. In the absence of Jacobian matrix inverse, the proposed control scheme shows better results and almost closes to the conventional operational-space controller's performance. The proposed scheme can be applied to any similar robotic system and is giving a generalised frame work for controlling mobile robotic systems.

REFERENCES

1. Tzafestas, S.G. Introduction to mobile robot control. *Elsevier,* 2014.
2. Chiaverini, S.; Oriolo, G; & Walker, I.D. Kinematically redundant manipulators. *In* Springer Handbook of Robotics, B. Siciliano and O. Khatib, 1st ed., Springer-Berlin, Germany: Springer, 2008 pp. 245-268. doi: 10.1007/978-3-540-30301-5_12
3. Atawnih, A; Papageorgiou, D; & Doulgeri, D. Kinematic control of redundant robots with guaranteed joint limit avoidance. *Rob. Auton. Sys.,* 2018, **99**, 110-120. doi: 10.1016/j.robot.2016.01.006
4. Caccavale, F. & Siciliano, B. Kinematic control of

redundant free-floating robotic systems. *J. Adv. Robotics,* 2012, **15**(4), 429-448.
doi: 10.1163/156855301750398347

5. Siciliano, B. A closed-loop inverse kinematic scheme for on-line joint-based robot control. *Robotica*, 1990, **8**(3), 231–243.
doi: 10.1017/S0263574700000096
6. Galicki, M. Generalized Kinematic control of redundant manipulators in robot motion and control. Krzyszt of R. Kozlowski, 1st ed. Springer-Verlag London 2007, 19-226.
doi: 10.1007/978-1-84628-974-3_19
7. Yao, X.Y.; Ding, HF;&Ge,MF. Task-space tracking control of multi-robot systems with disturbances and uncertainties rejection capability. *Nonlinear Dynamics,* 2018, **92**(4), 1649–1664.
doi: 10.1007/s11071-018-4152-y
8. Hong, S.; Lee, W.S.; Kang, Y.S. & Park, Y.W. Kinematic control algorithms and robust controller design for rescue robot. 14th International Conference on Control Automation and Systems (ICCAS) Seoul, South Korea, Oct. 22-25,2014, pp. 637-642.
doi: 10.1109/ICCAS.2014.6987858
9. Li, L.; Gruver, W.A.; Zhang, Q. & Yang, Z. Kinematic Control of Redundant Robots and the Motion Optimizability Measure. *IEEE Trans. Sys. Man and Cybernetics-Part B: Cybernetics,* 2001, **31**(1), 155-160.
doi: 10.1109/3477.907575
10. Koga, M.; Kosuge, K.; Furuta, K. & Nosaki, K. Coordinated motion control of robot arms based on the virtual internal model. *IEEE Trans. Robotics* Automation, 1992, **8**(1), 77-85.
doi: 10.1109/ROBOT.1989.100127
11. Ahmad, S. & Luo, S. Coordinated Motion Control of Multiple Robotic Devices for Welding and Redundancy Coordination through Constrained Optimization in Cartesian Space. *IEEE Trans. Robotics Automation*, 1989, **5**(4), 409-417.
doi: 10.1109/70.88055
12. Walker, M.W.; Kim, D. & Dionise, J. Adaptive coordinated motion control of two manipulator Arms. *In* Proc. IEEE International Conference on Robotics and Automation, Scottsdale, Arizoqa,1989 p. 1084-1090.
doi: 10.1109/ROBOT.1989.100125
13. Zhou, S.; Pradeep, Y.C.; Zhu, M.; Semprun, K.A. & Chen, P. Motion control of a nonholonomic mobile manipulator in task space, *Asian J. Control*, 2017, **20**(5), 1–10.
doi: 10.1002/asjc.1694
14. Chiaverini, S. Singularity-robust task-priority redundancy resolution for real-time kinematic control of robot manipulators. *IEEE Trans. Rob. Automation,* 1997, **13**(3), 398-410.
doi: 10.1109/70.585902
15. Nakanishi, J.; Cory, R.; Mistry, M; Peters, J. & Schaal, S. Comparative experiments on task space control with redundancy resolution. *In* IEEE/RSJ International Conference on Intelligent Robots and Systems; Edmonton, Alta., Canada, Aug. 2-6, 2005.
doi: 10.1109/IROS.2005.1545203
16. Sutton, R.S. & Barto, A.G. Reinforcement learning: An introduction MIT press, 2nd ed., Cambridge, Massachusetts London, England, 1998, ch.1, p.1-11.
17. Li, Z.; Zhao, T.; Chen, F.; Hu, F.; Su, C.Y. & Fukuda T. Reinforcement Learning of manipulation and grasping using dynamical movement primitives for a humanoid like mobile manipulator. *IEEE/ASME Trans. Mech.,*2017, **23**(1), 121-131.
doi: 10.1109/TMECH.2017.2717461
18. Althoefer, K.; Krekelberg, B.; Husmeier, D. & Seneviratne, L. Reinforcement learning in a rule-based navigator for robotic manipulators. *Neurocomput. Elsevier Sci.,* 2001, **37**, 51-70.
doi: 10.1016/S0925-2312(00)00307-6
19. Gibollet, R.P. & Rives, P. Applying visual servoing techniques to control a mobile hand-eye system. *In* IEEE International Conference of Robotics and Automation, Nagoya, Japan, May 21-27, 1995, pp. 166-171.
doi: 10.1109/ROBOT.1995.525280
20. Wang, Y.; Lang, H. &de Silva, C.W. A hybrid visual servo controller for robust grasping by wheeled mobile robots. *IEEE/ASME Trans. Mech.,* 2010, **15**(5), 757 – 769.
doi: 10.1109/TMECH.2009.2034740
21. Janabi-Sharifi, F.; Deng, L. & Wilson, W.L. Comparison of BASIC VISUAL SERVOING MEthods. *IEEE/ASME Trans.Mech.*, 2011, **16**(5), 967 – 983.
doi: 10.1109/TMECH.2010.2063710
22. Ben-Israel, A. & Greville T.N.E. Generalized Inverses: Theory and Applications, Springer New York, 2003.
23. Raja, R.; Dasgupta, B. & Dutta, A. Motion planning and redundancy resolution of a rover manipulator. *In* IEEE International WIE Conference on Electrical and Computer Engineering Dec. 19-20,2015, pp. 90-93.
doi: 10.1109/WIECON-ECE.2015.7444006
24. Yang, C.; Paul, G.; Ward, P.; & Liu, D. A path planning approach via task-objective pose selection with application to an inchworm-inspired climbing robot. *In* IEEE International Conference on Advanced Intelligent Mechatronics (AIM), Alberta, Canada, July 12-15, 2016,pp. 401-406.
doi: 10.1109/AIM.2016.7576800
25. Nandi, S. & Singh, T. Chance constraint based design of open-loop controllers for linear uncertain systems. *IEEE/ASME Trans. Mech.*, 2018, **23**(4), 1952 – 1963.
doi: 10.1109/TMECH.2018.2840107
26. Liu, T.; Lie, Y.; Han, L.; Xu, W. & Zou, H. Coordinated resolved motion control of dual-arm manipulators with closed chain. *Int. J. Adv. Robotic Sys.*, 2016, **13** (3), 1-14.
doi: 10.5772/63430
27. Liao, J.; Huang, F.; Chen, Z. & Yao, B. Optimization-based motion planning of mobile manipulator with high degree of kinematic redundancy. *Int J Intell Robot Appl*,2019,
doi: 10.1007/s41315-019-00090-7
28. Gill, R.; Kulić, D. & Nielsen, C. Path Following for Mobile Manipulators. In: Bicchi A., Burgard W. (eds) Robotics Research. Springer Proceedings in Advanced Robotics. *Springer, Cham.* 2018, **3.**
doi: 10.1007/978-3-319-60916-4_30

ACKNOWLEDGEMENT

This work was supported in part by the Department of Higher Education, Ministry of Human Resource Development (MHRD), India (Project No.:1-36/2016-PN-II).

CONTRIBUTORS

Ms Swati Mishra graduated in Automobile Engineering from Oriental Institute of Science & Technology, Bhopal, Madhya Pradesh, India, in 2010. She did her Master's in Specialising of Design and Thermal from Institute of Engineering, D.A.V.V Indore, in 2012. She is currently pursuing PhD in the Discipline of Metallurgy Engineering & Material Science at IIT Indore, India.
In the current study she carried out original draft preparation, collecting the data and editing of the paper.

Dr Santhakumar Mohan graduated from GCE Salem in 2003. He received his Master from GCT Coimbatore in 2005. He got his PhD (Robotics and Control) from IIT Madras in 2010. He worked as an Associate professor at IIT Indore till December 2018. Currently, he is working as an Associate professor at IIT Palakkad, India. He is holding visiting faculty positions at IISc Bangalore, India, RWTH Aachen, Germany and ECN, France.
In the current study, he guided in the formulation of concept and research objectives, analysis of data and execution of experiment and in preparation and editing of the draft

Dr Santosh Kumar Vishvakarma graduated from University of Gorakhpur in 1999. He received MSc in Electronics from DAVV Indore and MTech in Microelectronics from Punjab University in 2001 and 2003. He got PhD from IITRoorkee (Semiconductor Devices & VLSI Technology) in 2010. Currently, he is working as an Associate Professor in IIT Indore. His research interest includes Device Modelling and Circuit design.
In the current study, he guided in the preparation and editing of the draft.